Strongly correlated systems in atomic and condensed matter physics

Lecture notes

by Eugene Demler

ETH

November 23, 2023

Chapter 11

Fermion pairing close to Feshbach resonance. The BCS-BEC crossover.

11.1 BCS model in electron systems

We start by reviewing the BCS model of electron pairing in electron systems [13]. We consider a reduced Hamiltonian that includes terms which are decisive for pairing of fermions

$$\mathcal{H} = \sum_{k\sigma} \xi_k \, c^\dagger_{k\sigma} \, c_{k\sigma} + \sum_{kl} V_{kl} \, c^\dagger_{k\uparrow} \, c^\dagger_{-k\downarrow} \, c_{-l\downarrow} \, c_{l\uparrow} \tag{11.1}$$

Here $\xi_k = \frac{k^2}{2m} - \mu \equiv \epsilon_k - \mu$. The BCS wavefunction describes a many-body state with pairs of states $(k\uparrow, -k\downarrow)$ occupied or unoccupied as units in coherent manner. In the mean-field approximation we can describe such state by assigning finite expectation values to operators $c_{k\uparrow}\, c_{-k\downarrow}$. The mean-field Hamiltonian is given by

$$\mathcal{H} = \sum_{k\sigma} \xi_k \, c^\dagger_{k\sigma} \, c_{k\sigma} + \sum_{kl} V_{kl} \, (\, c^\dagger_{k\uparrow} \, c^\dagger_{-k\downarrow} \, b_l \, + \, b^*_k \, c_{-l\downarrow} \, c_{l\uparrow} \, - b^*_k b_l \,) \tag{11.2}$$

Here b_k are numbers, not operators, which need to be determined self-consistently. We define

$$\Delta_k = \sum_l V_{kl} \, b_l \, = \, \sum_l V_{kl} \, \langle c_{-l\downarrow} \, c_{l\uparrow} \, \rangle \tag{11.3}$$

Then

$$\mathcal{H}_{\rm MF} = \sum_{k\sigma} \xi_k \, c^\dagger_{k\sigma} \, c_{k\sigma} + \sum_k (\, \Delta_k \, c^\dagger_{k\uparrow} \, c^\dagger_{-k\downarrow} \, + \, \Delta^*_k \, c_{-k\downarrow} \, c_{k\uparrow} - \Delta_k \, b^*_k \,) \tag{11.4}$$

Fermionic part of the Hamiltonian can be diagonalized by the Bogoliubov transformation. In simple s-wave superconductors Δ_k should have the same phase for all k, although the actual value of the phase is not important. For simplicity we set Δ_k to be real

$$\begin{aligned} c_{k\uparrow} &= u_k \gamma_{k\uparrow} + v_k \gamma^\dagger_{-k\downarrow} \\ c_{-k\downarrow} &= -v_k \gamma^\dagger_{k\uparrow} + u_k \gamma_{-k\downarrow} \end{aligned} \tag{11.5}$$

When coefficients u_k and v_k satisfy

$$\begin{aligned} 2\xi_k u_k v_k &+ \Delta_k u_k^2 - \Delta_k v_k^2 = 0 \\ u_k^2 &+ v_k^2 = 1 \end{aligned} \tag{11.6}$$

we find that off-diagonal terms in the fermionic Hamitlonian vanish and we obtain

$$\mathcal{H}_{\rm MF} = \sum_k E_k \, (\, \gamma^\dagger_{k\uparrow} \gamma_{k\uparrow} \, + \, \gamma^\dagger_{k\downarrow} \gamma_{k\downarrow} \,) \tag{11.7}$$

with

$$E_k = \sqrt{\xi_k^2 + \Delta_k^2} \tag{11.8}$$

From equation (10.3) we obtain self-consistency condition

$$\Delta_k \, = \, - \sum_{k'} V_{kk'} \, \langle c_{-k'\downarrow} \, c_{k'\uparrow} \rangle \, = \, - \sum_{k'} V_{kk'} \, u_{k'} \, v_{k'} \, \langle \, (\, 1 \, - \, \gamma^\dagger_{k'\uparrow} \gamma_{k'\uparrow} \, - \gamma^\dagger_{k'\downarrow} \gamma_{k'\downarrow} \,) \, \rangle \tag{11.9}$$

At finite temperature we have $\langle \, \gamma^\dagger_{k'\sigma} \, \gamma_{k'\sigma} \, \rangle \, = f(E_{k'}) \equiv 1/(1 + e^{\beta E_{k'}})$ so

$$\Delta_k \, = \, - \sum_{k'} V_{kk'} \, \frac{\Delta_{k'}}{2E_{k'}} \, \tanh(\frac{\beta E_{k'}}{2}) \tag{11.10}$$

There is also self-consistency equation on the chemical potential

$$n = \sum_{k\sigma} \langle \, c^\dagger_{k\sigma} \, c_{k\sigma} \, \rangle \, = \, 2 \sum_k v_k^2 - \sum_{k\sigma} (v_k^2 - u_k^2) \, \langle \, \gamma^\dagger_{k\sigma} \, \gamma_{k\sigma} \, \rangle \tag{11.11}$$

In the BCS model of superconductivity in metals $V_{kk'}$ is constant but there is energy cut-off $|\xi_k| \leq \omega_D$, where ω_D is the phonon Debye frequency. Then

$$-\frac{1}{V} = \frac{1}{2} \sum_{|\xi_k| \leq \omega_D} \frac{\tanh(\frac{\beta E_{k'}}{2})}{E_k} \tag{11.12}$$

At $T = 0$ we find

$$-\frac{1}{V} = \frac{1}{2} \sum_{|\xi_k| \leq \omega_D} \frac{1}{E_k} \tag{11.13}$$

Assuming $\omega_D << E_F$ so variations of the density of states with energy can be neglected, one finds

$$\begin{aligned} \Delta &= \frac{\omega_D}{\sinh\left[\frac{1}{N(0)V}\right]} \simeq 2\omega_D\, e^{-\frac{1}{N(0)V}} \\ T_c &= 1.14\omega_D\, e^{-\frac{1}{N(0)V}} \end{aligned} \tag{11.14}$$

Here $N(0)$ is the density of states at the Fermi energy.

11.2 BCS for ultracold atoms

When extending BCS approach to ultracold atoms (see Refs. [2, 11, 12] for review), we should remember that there is no energy cut-of such as ω_D. There is only ultraviolet cut-off in equation (10.13) when $|k| \leq R^{-1}$. Our approach is again to trade bare interaction for the scattering length. We have

$$\frac{m}{4\pi a_s} = \frac{1}{V} + \sum_{|k|\leq R^{-1}} \frac{m}{k^2} \tag{11.15}$$

We can combine equation (10.15) with

$$-\frac{1}{V} = \frac{1}{2} \sum_{|k|\leq R^{-1}} \frac{1}{E_k} \tag{11.16}$$

to obtain

$$-\frac{m}{4\pi a_s} = \frac{1}{2} \sum_k \left(\frac{1}{E_k} - \frac{m}{k^2} \right) \tag{11.17}$$

The last integral over k converges and so we sent the cut-off R^{-1} to infinity.

11.3 Mathematical details

When analyzing equations (10.11), (10.17) it is convenient to define dimensionless quantities [7]

$$\begin{aligned} x^2 &= \frac{k^2}{2m}\frac{1}{\Delta} \\ x_0 &= \frac{\mu}{\Delta} \\ \xi_x &= \frac{\xi_k}{\Delta} = x^2 - x_0 \\ E_x &= \frac{E_k}{\Delta} = \sqrt{\xi_x^2 + 1} \end{aligned} \tag{11.18}$$

We can rewrite (10.11), (10.17) as

$$\begin{aligned} -\frac{1}{a_s} &= \frac{2}{\pi}(2m\Delta)^{1/2} I_1(x_0) \\ n &= \frac{1}{2\pi^2}(2m\Delta)^{3/2} I_2(x_0) \end{aligned} \tag{11.19}$$

Here

$$\begin{aligned} I_1(x_0) &= \int_0^\infty dx\, x^2 (\frac{1}{E_x} - \frac{1}{x^2}) \\ I_2(x_0) &= \int_0^\infty dx\, x^2 (1 - \frac{\xi_x}{E_x}) \end{aligned} \tag{11.20}$$

The last two integrals can be written as

$$\begin{aligned} I_1(x_0) &= 2(x_0 I_6(x_0) - I_5(x_0)) \\ I_2(x_0) &= \frac{2}{3}(x_0 I_5(x_0) + I_6(x_0)) \end{aligned} \tag{11.21}$$

where

$$\begin{aligned} I_5(x_0) &= (1+x_0^2)^{1/4} E(\frac{\pi}{2}, \kappa) - \frac{1}{4x_1^2(1+x_0^2)^{1/4}} F\frac{\pi}{2}, \kappa) \\ I_6(x_0) &= \frac{1}{2(1+x_0^2)^{1/4}} F(\frac{\pi}{2}, \kappa) \\ x_1^2 &= \frac{(1+x_0^2)^{1/2} + x_0}{2} \\ \kappa^2 &= \frac{x_1^2}{(1+x_0^2)^{1/2}} \end{aligned} \tag{11.22}$$

and we used elliptic functions

$$\begin{aligned} F(\alpha, \kappa) &= \int_0^\alpha d\phi \frac{1}{\sqrt{1 - \kappa^2 \sin^2\phi}} \\ E(\alpha, \kappa) &= \int_0^\alpha d\phi \sqrt{1 - \kappa^2 \sin^2\phi} \end{aligned} \tag{11.23}$$

11.3.1 BCS limit

When scattering length is small and negative we have $x_0 >> 1$. In this limit we can approximate

$$\begin{aligned} I_5(x_0) &\approx \sqrt{x_0} \\ I_6(x_0) &\approx lnx_0/2\sqrt{x_0} \end{aligned} \tag{11.24}$$

Then we find

$$\begin{aligned} \frac{\Delta_0}{E_F} &= \frac{1}{x_0} \\ \frac{\mu}{E_F} &= 1 \\ \frac{1}{k_F a_s} &= -\frac{2}{\pi}\ln x_0 \end{aligned} \tag{11.25}$$

So we find the BCS like expression

$$\Delta_{\rm gap} = \Delta = \frac{8}{e^2} E_F \, e^{\frac{\pi}{2k_F a}} \tag{11.26}$$

11.3.2 BEC Regime

When scattering length is positive and large we have essentially a weakly interacting gas of molecules. In this regime $x_0 < 0$ and $|x_0| >> 1$. Then

$$\begin{aligned} \kappa^2 &= \frac{1}{4x_0^2} \\ I_5(x_0) &\approx \frac{\pi}{16|x_0|^{3/2}} \\ I_6(x_0) &\approx \frac{\pi}{4|x_0|^{1/2}} \end{aligned} \tag{11.27}$$

This gives us

$$\begin{aligned} \frac{\Delta}{E_F} &= \left(\frac{16}{3\pi}\right)^{2/3} |x_0|^{1/3} \\ \frac{\mu}{E_F} &= -\left(\frac{16}{3\pi}\right)^{2/3} |x_0|^{4/3} \\ \frac{1}{k_F a_s} &= \left(\frac{16}{3\pi}\right)^{2/3} |x_0|^{2/3} \end{aligned} \tag{11.28}$$

We find precisely what we expect

$$\mu = -\frac{\hbar^2}{2ma^2}. \tag{11.29}$$

For the quasiparticle gap we have $\Delta_{\rm gap} = \sqrt{\Delta^2 + \mu^2}$. Since $\Delta << |\mu|$ we find $\Delta_{\rm gap} \approx \frac{\hbar^2}{2ma^2}$.

11.3.3 Evolution of quasiparticles in the BCS-BEC crossover

Nontrivial change in the dispersion of quasiparticles across the BCS-BEC crossover is shown in fig. 10.1. The minimum in the quasiparticle dispersion is at k_F in the BCS regime and at $k = 0$ on the BEC side.

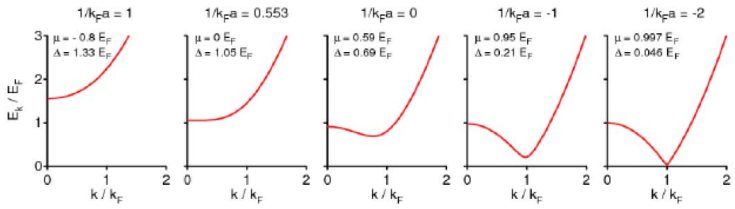

Figure 11.1: Evolution of fermionic quasiparticles across the BCS-BEC crossover. Figure taken from [12].

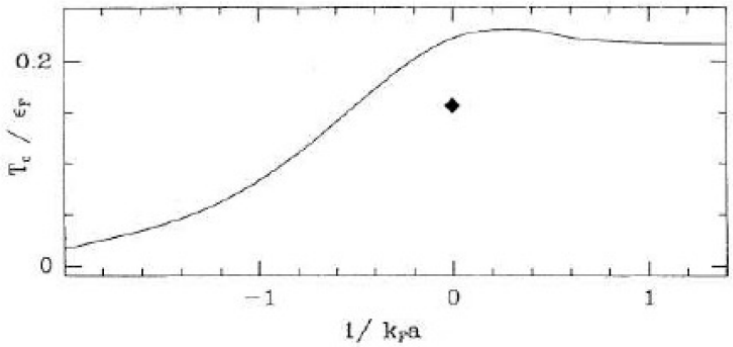

Figure 11.2: Transition temperature as a function of the scattering length across the BCS-BEC crossover, calculated using mean-field theory. The diamond corresponds to the Monte Carlo simulation at unitarity by Burovski et al. Figure taken from [11].

11.3.4 Phase Diagram

One can also use this approach to calculate $\Delta(T)$. It is natural to define Tc as the highest temperature at which $\langle\Delta\rangle \neq 0$.

$$T_c^{\mathrm{BCS}} = \frac{8e^{\gamma_E}}{\pi e^2} E_F e^{-\frac{\pi}{2}\frac{1}{k_F|a_s|}} \tag{11.30}$$

with $\gamma_E = 0.57772...$

$$T_c^{\mathrm{BEC}} = 3.31\frac{\hbar^2 n_B^{2/3}}{m_B} = 0.218 E_F \tag{11.31}$$

Figure 10.2 shows Tc across the entire Feshbach resonance region. Note a small increase of Tc as the system approaches unitarity from the BEC side. This can be understood as a result of repulsive ineraction between molecules. One known artifact of the mean-field approach is the prediction of the first order transition into the superfluid state on the BEC side of the phase diagram, see [8] and fig. 10.3.

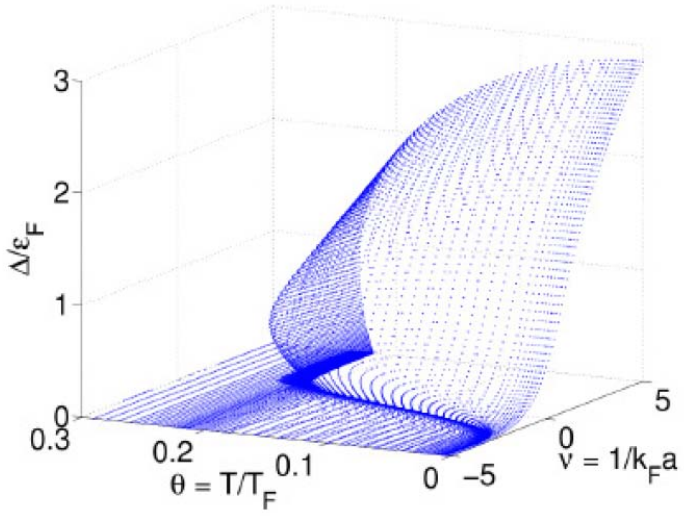

Figure 11.3: Order parameter as a function of the interaction strength and temperature. On the BEC side the order parameter exhibits multivalued behavior near Tc characteristic of the first order transition. Figure taken from [8].

11.4 BCS Wavefuncion

Mean-field solution (10.4) is equivalent to the BCS wavefunction (at $T = 0$)

$$|\Psi_{\text{BCS}}\rangle = \prod_k (u_k + v_k c^\dagger_{k\uparrow} c^\dagger_{-k\downarrow})|0\rangle \tag{11.32}$$

The BCS ground state derived in the last section should be the vacuum of the Bogoliubov quasiparticles $\gamma_{k\sigma}$. Using equations (10.5) we can verify that $\gamma_{k\sigma}|\Psi\rangle = 0$.

We can also write equation (10.32) as

$$|\Psi_{\text{BCS}}\rangle = \prod_k u_k \, e^{\sum_k \frac{v_k}{u_k} c^\dagger_{k\uparrow} c^\dagger_{-k\downarrow}} |0\rangle \tag{11.33}$$

The part of $|\Psi_{\text{BCS}}\rangle$ that contains precisely N particles is

$$\left[\sum_k \frac{v_k}{u_k} c^\dagger_{k\uparrow} c^\dagger_{-k\downarrow}\right]^{N/2} |0\rangle \tag{11.34}$$

This is a condensate of Cooper pairs with the wavefunction

$$\phi(r) = \int d^3r \, e^{i\vec{k}\vec{r}} \frac{v_{\vec{k}}}{u_{\vec{k}}} \tag{11.35}$$

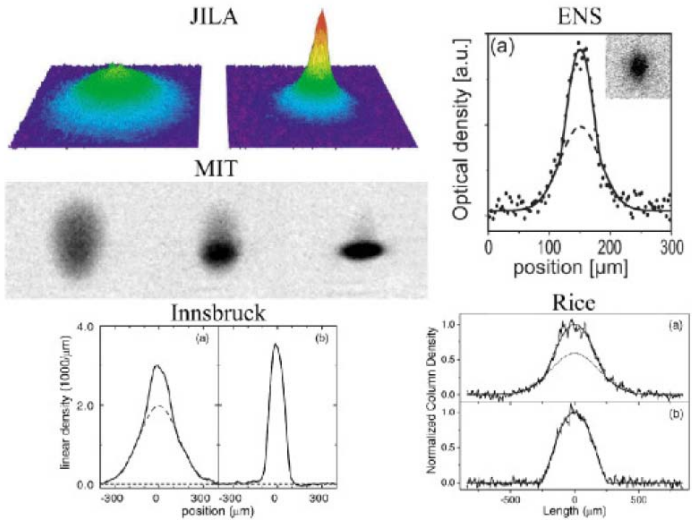

Figure 11.4: Observation of Bose-Einstein condensation of molecules. This collection of images shows bimodal density distributions in both in-situ profiles (Innsbruck and Rice) and after expansion (JILA, MIR, ENS). Figure taken from [12].

Far on the BEC side

$$\phi(r) \sim \frac{1}{\sqrt{2\pi a r}}\, e^{-r/a} \tag{11.36}$$

11.5 Experimental observation of superfluidity in fermionic systems

On the BEC side of the Feshbach resonance the superfluid state of tightly bound molecules should be very similar to a condensate of Bosonic atoms. Hence one can look for standard signatures of superfluidity: bimodal density distributions both inside the trap and after some expansion. Observation of vortex lattice is another important signature of superfluidity.

11.5.1 Projection experiments

On the BCS side of the Feshbach resonance Cooper pairs exist only as a many-body effect. In the dilute limit there are only inidividual atoms so TOF expansion unbinds the molecules. To demonstrate pairing in this regime one should convert Cooper pairs into molecules first and expand after that. This can be achieved by quickly sweeping the magnetic field to the BEC side of the resonance [12, 3]. We will discuss only the simplest model of such experiments, in which we assume that the sweep rate is very large, and we can treat these experiments as a

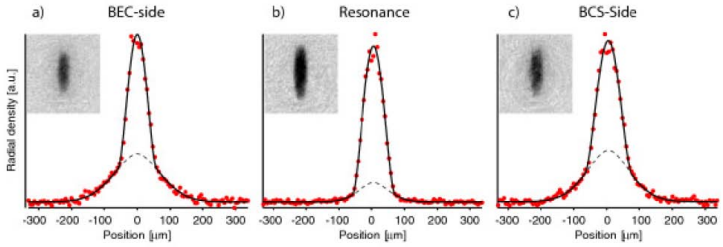

Figure 11.5: Experimental demonstration of fermion pair condensates. Bimodal distribution after short expansion. This figure shows axial density of the atomic cloud after switching off the optical trap, a rapid ramp to zero field, further short expansion, and dissociation of the resulting molecules by ramping back across resonance. Ramping to zero field across the BEC regime converts Cooper pairs from the BCS/unitary regimes into Feshbach molecules (see section 10.5.1). These molecules then expand without dissociating. Figure taken from [12].

projection of the many-body wavefunction. In analyzing real experiments there may be important corrections due to finite rate of the magnetic field sweep[1].

We can express the operator that creates a molecule in the final point of the projection experiment as

$$b_q^\dagger = \int dk\, \phi_f(k)\, c^\dagger_{\frac{q}{2}+k\uparrow}\, c^\dagger_{\frac{q}{2}-k\downarrow} \tag{11.37}$$

Here q is the momentum of the molecule and $\phi_f(k)$ is the molecular wavefunction. The number of molecules with momentum q is $n_m(q) = b_q^\dagger b_q$. For a projection type experiment we can calculate the number of molecules by taking the expectation value of $n_m(q)$in the initial state

$$n_m(q) = \int dk\, dk'\, \phi_f^*(k)\, \phi_f(k')\, \langle c^\dagger_{\frac{q}{2}+k\uparrow}\, c^\dagger_{\frac{q}{2}-k\downarrow} c_{\frac{q}{2}-k'\downarrow}\, c_{\frac{q}{2}+k'\uparrow} \rangle \tag{11.38}$$

We take the initial state to be of the type (10.32). Direct calculation gives

$$n_m(q) \;=\; \delta(q)\, |\int dk\, \phi(k)\, \langle\, c^\dagger_{k\uparrow}\, c^\dagger_{-k\downarrow}\, \rangle\, |^2 \;+\; \int dk |\phi(k)|^2\, \langle n_{\frac{q}{2}+k\uparrow} \rangle \langle n_{\frac{q}{2}-k\downarrow} \rangle \tag{11.39}$$

The first term in (10.39) measures the number of molecules created in the condensate, i.e. in the $q = 0$ state. This contribution is present only when there is coherent pairing in the initial state and $\langle\, c^\dagger_{k\uparrow}\, c^\dagger_{-k\downarrow}\, \rangle \neq 0$. Not surprisingly this term is proportional to the overlap of the wavefunctions for Cooper pairs and the final state molecules. The second term in (10.39) gives the number of non-condensate molecules produced after the sweep. This contribution is present even when the initial state is not paired. It reflects a finite probability of atoms to be close to each other in the initial state, so that the magnetic field sweep can turn them into molecules. In the simplest approximation one can take the wavefunction of the final state molecules to be constant for $k < 1/a_*$ and zero

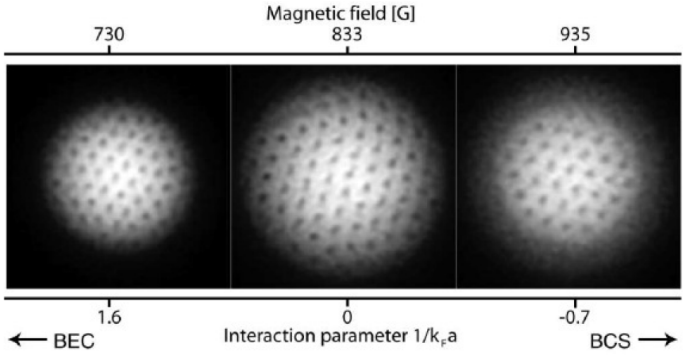

Figure 11.6: Observation of vortices in a strongly interacting Fermi gas. Superfluidity, coherence, and vortex lattice were established at different value of the magnetic field. magnetic field was ramped to the BEC side for imaging. Figure taken from [12].

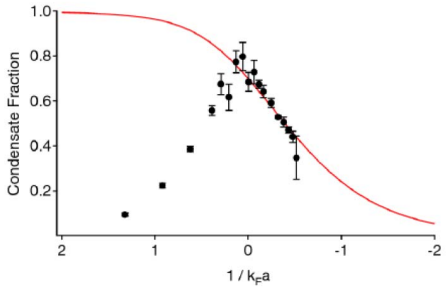

Figure 11.7: Condensate fraction as a function of interaction strength. Comparison of theory and experiments. Figure taken from [12]. On the BEC side heating due to vibrational relaxation leads to the rapid decay of the condensate.

otherwise. Here a_* is the size of the molecule. Note that this is not the size of the closed channel bound state but the size of the Feshbach molecules including the open channel, which should be of the order of the scattering length. For the coherent part we find

$$\frac{N_0}{V} = \frac{6a_*^3}{(2\pi)^3}\int_0^{a_*^{-1}} \frac{dk\, k^2\, \Delta/2}{\sqrt{\Delta^2+\xi_k^2}} = \frac{9n}{8}\left(\frac{\Delta}{E_f}\right)^2 k_f\, a_* \tag{11.40}$$

Here n is the density of atoms. It is easy to understand why the final result is proportional to $|\Delta|^2$ and a_*. The Cooper pair wavefunction goes as $\phi_c(r) \sim \Delta/r$ at short distances. Molecular wavefunction is $\phi_m \sim a_*^{-3/2}$ for $r < a_*$. Hence $|\langle\phi_c|\phi_m\rangle|^2 \sim |\Delta|^2\, a_*$. Figure 10.7 shows comparison of this simple model with the experimental results.

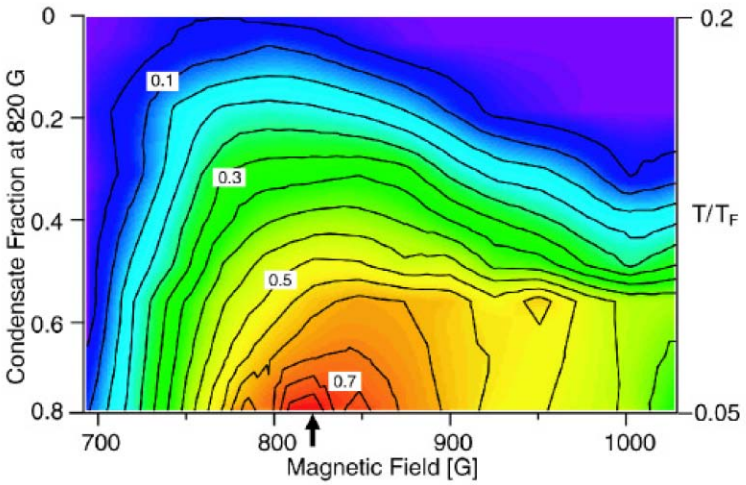

Figure 11.8: Condensate fraction as a function of magnetic field and temperature in experiments on ^{6}Li. Arrow marks the position of the Feshbach resonance. Figure taken from [12].

11.5.2 Observing pairing in noise correlations

Noise correlations analysis that we discussed in Chapter 8 can be also used to probe pairing. We consider TOF experiments with fermionic atoms on the BCS side or at unitarity. Ballistic (collision free) expansion can be achieved by ramping the magnetic field to the weakly interacting regime. After sufficiently long expansion times we find real space distributions of atoms reflecting momentum occupations $n_{k\sigma} = c^\dagger_{k\sigma} c_{k\sigma}$. In the ideal case of zero temperature and uniform system one could argue that smearing of $n_{k\sigma}$ should be a signature of Cooper pairing. In Fermi liquid states one expects to find a discontinuity in the occupation number at the Fermi momentum. However finite temperature and inhomogeneous density can also smear the Fermi surface. A more striking feature of pairing is correlations in the occupation numbers. The BCS wavefunction (10.32) demonstrates that occupation of the states $k\uparrow$ and $-k\downarrow$ are perfectly correlated. Each of these states can be either occupied or not (e.g. at the Fermi momentum the occupation probability is 50%). However these states are either occupied or empty simultaneously. If one detects an atom in state $k\uparrow$, there must be an atom in a state $-k\downarrow$. If there was no atom in the sate $k\uparrow$, there should be no atom in the state $-k\downarrow$. A proof of concept experiment was done by M. Greiner et. al. [6] and is summarized in Fig. 10.9. This experiment was done on the BEC side with an RF pulse was applied to dissociate molecules.

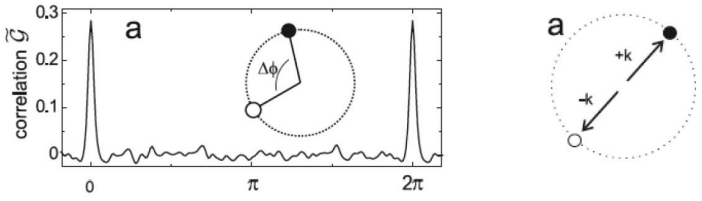

Figure 11.9: Pairing correlations in a condensate of Fermi pairs. Correlations in the TOF images reflect pairing of k and $-k$ states. Figure taken from [12].

11.6 RF spectroscopy

11.6.1 Momentum unresolved RF spectroscopy

The idea of RF spectroscopy is to transfer a small number of atoms into another hyperfine state by applying an electro-magnetic pulse at radio frequencies. Typically one measures the number of atoms transferred as a function of the pulse frequency. If the number of transferred atoms is sufficiently small one can use linear response theory to describe the process of the atom transfer.

Let $\mathcal{H}_{\rm syst}$ be the Hamiltonian that describes two interacting species of fermions $c_{k\sigma}$, which we assume to be given in the grand canonical ensemble. We take the RF pulse that couples $c_{k\uparrow}$ fermions to the third state f_k.

$$\mathcal{H}_{\rm RF} = \sum_k (\omega_0 + \frac{k^2}{2m}) f_k^\dagger f_k + \Omega_R \sum_k (e^{-i\omega t} f_k^\dagger c_{k\uparrow} + e^{i\omega t} c_{k\uparrow}^\dagger f_k) \qquad (11.41)$$

Here Ω_R is the Rabi frequency controlled by the intensity of the pulse, ω_0 is the energy of the f fermions relative to $c_\uparrow$. Note that the RF pulse does not change momenta of fermions since photon momentum is negligible.

Within linear response theory one can use Fermi's golden rule to calculate the rate of the fermion transfer

$$\begin{aligned} \frac{I(\omega)}{2\pi\Omega_R^2} &= \sum_n |\langle n|A^\dagger|0\rangle|^2 \, \delta(\omega - (\omega_{n0} - \mu)) \\ A^\dagger &= \sum_k f_k^\dagger c_k \end{aligned} \qquad (11.42)$$

Here $\omega_{n0} = E_n - E_0$ with E_n being the energy of state $|n\rangle$, in which one fermion has been transferred into the f state, and E_0 being the energy of the initial state. It may seem surprising that formula (10.42) has the chemical potential term in the delta function for the energy. This is is because in calculating E_n and E_0 we want to use the grand canonical representation of $\mathcal{H}_{\rm syst}$, which includes the $-\mu N$ term. The actual physical frequency measured in experiments needs to be calculated using the canonical form of the Hamiltonian. However we know that state $|n\rangle$ will have one fermion transferred from the $c_\uparrow$ to f state, hence we can

simply add the $-\mu$ term in equation (10.42) to compensate for the use of the grand canonical ensemble.

It may seem awkward that we choose to work in the grand canonical ensemble and then compensate for it by adding μ to the Fermi's golden rule. The motivation for doing this is that in the case of many-body pairing we know how to solve the problem in the grand canonical ensemble. For example, Bogoliubov operators $\gamma^\dagger_{k\sigma}$ (see equation (10.5)) create excited states in the BCS Hamiltonian. The energy of these excited states, which we obtained earlier, corresponds to the grand-canonical ensemble representation of the system.

Let us start with the simplest case of noninteracting fermions. Then state $|n\rangle$ corresponds to moving one of the fermions from the Fermi sea of $c_{k\uparrow}$ into f_k state. The energy of this state is $E_n = (\omega_0 + k^2/2m) + (\mu - k^2/2m)$. Here $\omega_0 + k^2/2m$ comes from adding a fermion into state f_k, and $\mu - k^2/2m$ comes from creating a hole excitation in the Fermi sea of $c_{k\uparrow}$ (remember that we work in the grand canonical ensemble). Hence in this case we find $\omega_{n0} = \omega_0 + \mu$ regardless of the momentum of the fermion which has been transferred. For the RF spectrum we find $I(\omega) = 2\pi\Omega_R^2 n\delta(\omega - \omega_0)$, where n is the density of fermions.

Let us now consider a paired state described by the BCS mean-field theory. Excited states $|e_k\rangle$ should be of the form

$$|e_k\rangle = \gamma^\dagger_{-k\downarrow} f^\dagger_k \,|\Psi_{\rm BCS}\,\rangle \tag{11.43}$$

The energy of this state (in the grand canonical ensemble again) is $E_k + \omega_0 + \frac{k^2}{2m}$. Using Bogoliubov transformation formulas (10.5) we easily find that the matrix element ${}_k\langle n|A^\dagger|0\rangle = v_k$, hence

$$\frac{I(\omega)}{2\pi\Omega_R^2} = \int_k v_k^2 \delta(\omega - (E_k + \frac{k^2}{2m} + \omega_0 - \mu)) \tag{11.44}$$

We recall that $\xi_k = \frac{k^2}{2m} - \mu$ and using the usual rules of δ-functions we can rewrite the last formula as

$$\frac{I(\omega)}{2\pi\Omega_R^2} = \int_{\xi_k} \rho(\xi_k)\,\delta(\omega - (E_k + \xi_k + \omega_0)) = \rho(\xi_k)\frac{v_k^2}{2u_k^2}|_{E_k + \frac{k^2}{2m} - \mu + \omega_0 = \omega} \tag{11.45}$$

In writing the last equation we used $2u_k^2 = (1 + \xi_k/E_k)$.

The smallest energy for which we find a nonzero $I(\omega)$ comes from $k = 0$ in (10.45). So $I(\omega)$ starts from the frequency $\omega_{\rm th}$

$$\omega_{\rm th} - \omega_0 = \sqrt{\mu^2 + \Delta^2} - \mu \tag{11.46}$$

We have the following limiting cases

$$\omega_{\rm th} - \omega_0 = \begin{array}{c} \frac{\Delta^2}{2E_F} \text{ in the BCS limit} \\ 0.31\,\Delta \text{ on resonance} \\ |E_{\rm B}| = \frac{\hbar^2}{ma^2} \text{ in the BEC limit} \end{array} \tag{11.47}$$

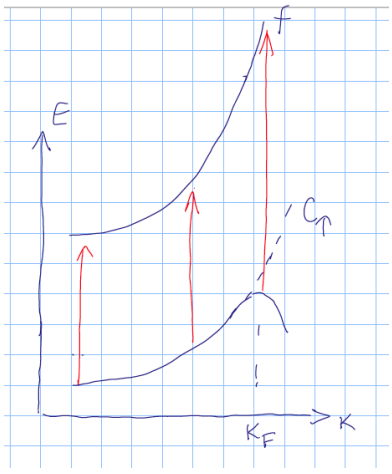

Figure 11.10: Schematic representation of RF experiments in the paired states. The RF pulse changes the hyperfine state of all atoms without affecting their momenta.

The most important feature of RF spectra in (10.47) is the presence of the pairing gap. Finite energy is required to break pairs into individual atoms. In the BEC limit the value of $\omega_{\rm th}$ is simply the binding energy. The BCS value of $\omega_{\rm th}$ is more surprising. Naively RF experiments appear similar to tunneling experiments in electron systems. However the gap observed in tunneling experiments (which are naturally in the BCS regime) is Δ. It is useful to discuss what causes the difference. In tunneling experiments momentum is not conserved. So the smallest energy required for taking an electron out corresponds to creating a quasiparticles at momentum near k_F and requires energy Δ. The crucial component of RF spectroscopy is conservation of momentum. As a result RF spectra start with fermions at $k = 0$, which are only weakly affected by pairing in the BCS regime. This is shown schematically in fig. 10.10.

In the discussion so far we assumed that state f does not interact with states $c_{k\sigma}$. In many experimental systems, however, this interaction is not negligible. It often leads to strong modifications of the RF spectra. For example, let us assume that state f interacts with state $c_\downarrow$ precisely the same way as the state $c_\uparrow$. Then the RF pulse should rotate $c_{k\uparrow}$ fermions into f_k, without affecting the nature of the paired state. So the RF spectrum should look like a δ-function with $\omega = \omega_0$ [14]. For example, RF spectra measured originally by the Innsbruck group, see fig. **??**, appear much sharper than theoretical predictions shown in fig. 10.11. More recent experiments tried to minimize effects of finite state interactions, see fig. 10.13.

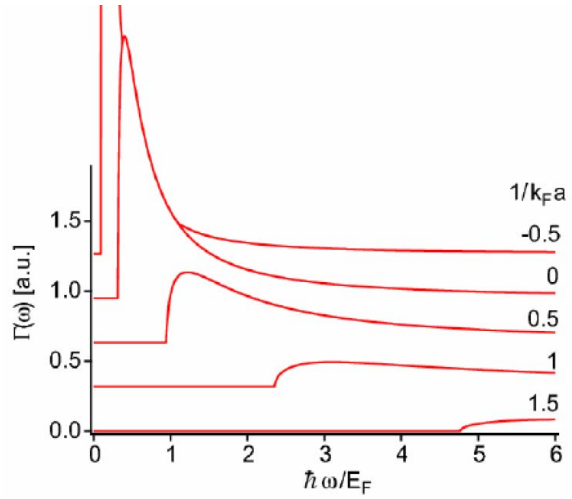

Figure 11.11: RF spectra across the BCS-BEC crossover. Figure taken from [12].

11.6.2 Momentum resolved RF spectroscopy. Photoemission

D. Jin and collaborators developed an interesting refinement of the RF spectroscopy technique[10]. They went beyond measuring the total number of atoms created by the RF pulse, by following the RF pulse with the TOF expansion of the atoms. This allowed them to measure the number of excited f_k atoms as a function of momentum k[10]. These experiments provide cold atoms analogue of photoemission spectroscopy in electron systems[4]. The simplest way to understand such experiments is to think of energy conservation. For a given value of momentum k we know the RF frequency ω_k, which converts $c_{k\uparrow}$ into f_k. We also know the kinetic energy of fermions in the final state $E_{\text{final}\,k} = \omega_0 + \frac{k^2}{2m}$. Then from energy conservation we can calculate the energy of fermions in the initial state, $E_{\text{init}\,k} = E_{\text{final}\,k} - \omega_k$. We can also think abut it as finding the energy of creating a hole excitation in the interacting many-body system. Fig. 10.14 shows results of photoemission experiments across the BCS-BEC crosover.

11.7 Problems to Chapter 10

Problem 1.

Consider mean-field equations (10.11) and (10.17) for the paired state in the BCS-BEC crossover regime at $T = 0$. These equations need to be solved for the chemical potential μ and the order parameter Δ.

a) Show that in the BCS regime of negative small a_s we find equations (10.25), (10.26).

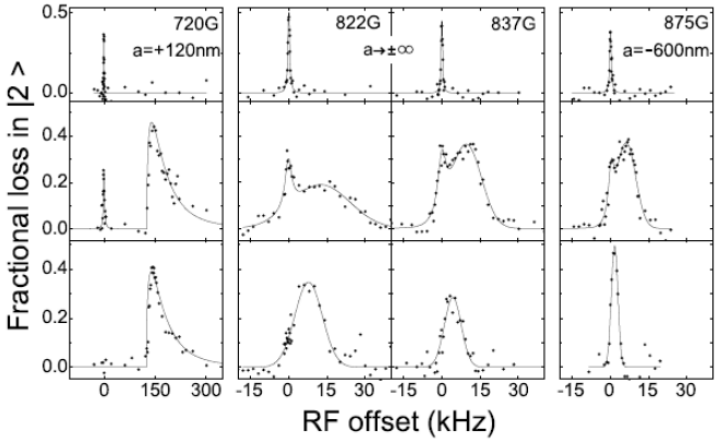

Figure 11.12: Experimentally measured RF spectra across the BCS-BEC crossover. Upper plots correspond to $T/T_F \approx 6$, middle plots to $T/T_F \approx 0.5$, bottom plots to $T/T_F < 0.2$. FInal state interactions are important for interpreting these results. Figure taken from [5].

b) Show that in the BEC regime of positive small a_s we find equation (10.29) and that $\Delta << |\mu|$

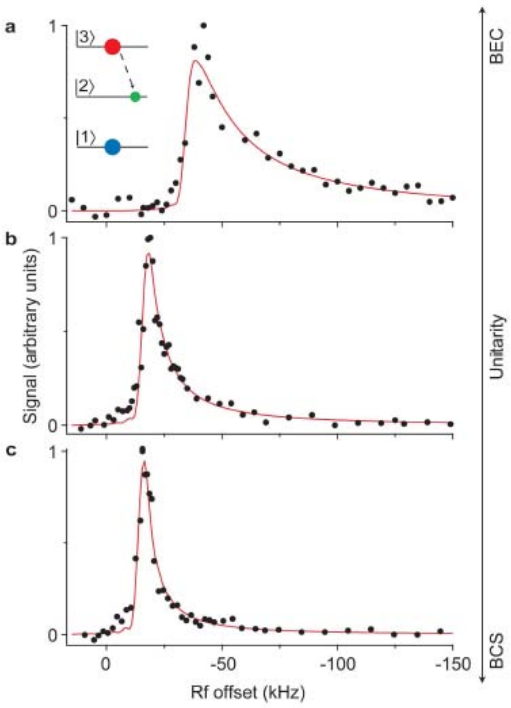

Figure 11.13: Experimentally measured RF spectra across the BCS-BEC crossover. Interaction strengths (for $c_\downarrow - f$ and $c_\downarrow - c_\uparrow$ respectively), $1/k_F a_i$, are (a) 0.2, 0.4; (b) 0.1, 0; (c) 0.1, -0.3. Figure taken from [9].

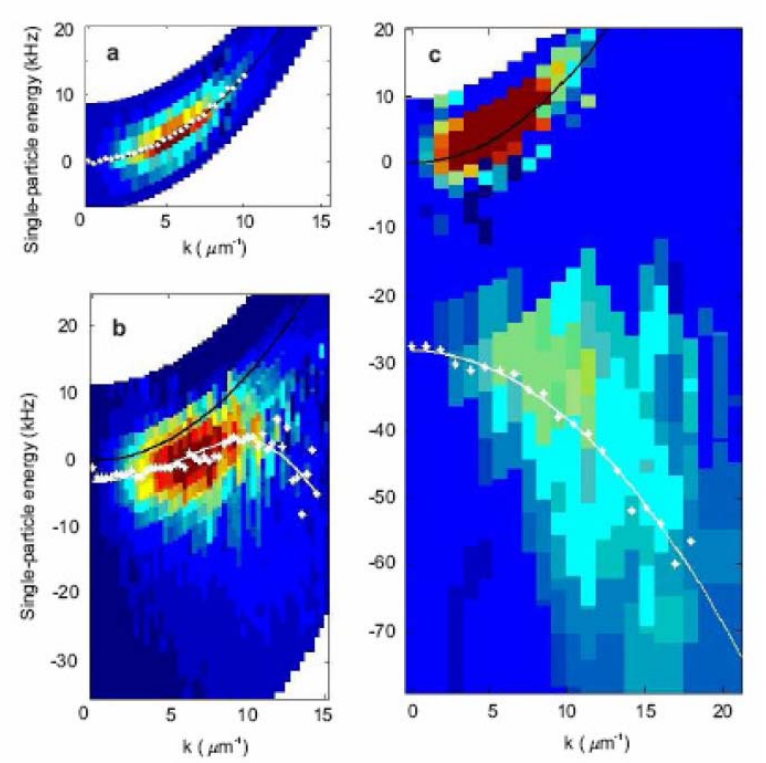

Figure 11.14: Photoemission in ultracold fermions. Plot a is for weakly interacting gas, plot b is on resonance and $T \approx T_c$, plot c is on the BEC side, $k_F a \approx 1$. The upper feature on plot c is attributed to unpaired fermions. Figure taken from [10].

Bibliography

[1] Ehud Altman and Ashvin Vishwanath. Dynamic projection on feshbach molecules: A probe of pairing and phase fluctuations. *Phys. Rev. Lett.*, 95(11):110404, Sep 2005.

[2] Immanuel Bloch, Jean Dalibard, and Wilhelm Zwerger. Many-body physics with ultracold gases. *Rev. Mod. Phys.*, 80(3):885–964, Jul 2008.

[3] Diener and Ho. *arXiv:cond-mat/0404517*, 2004.

[4] A. Damascelli et al. *Rev. Mod. Phys.*, 75:473, 2002.

[5] C. Chin et al. *Science*, 305:1128, 2004.

[6] M. Greiner et al. *Phys. Rev. Lett.*, 94:110401, 2005.

[7] Marini et al. *Eur.J. Phys. B*, 1:151, 1998.

[8] R. Haussmann et al. *Phys. Rev. A*, 75:23610, 2007.

[9] Schunck et al. *Nature*, 454:739, 2008.

[10] Stewart et al. *Nature*, 454:744, 2008.

[11] Stefano Giorgini, Lev P. Pitaevskii, and Sandro Stringari. Theory of ultracold atomic fermi gases. *Rev. Mod. Phys.*, 80(4):1215–1274, Oct 2008.

[12] W. Ketterle and M. Zwierlein. *Proceedings of the International School of Physics "Enrico Fermi", Course CLXIV, Varenna, arXiv:0801.2500*, 2000.

[13] J.R. Schrieffer. *Theory of Superconductivity.* Addison-Wesley Publishing Company, 1983.

[14] Z. Yu and G. Baym. *Phys. Rev. A*, 73:63601, 2006.